Cytochrome *c*–Lipid Interactions Studied by Resonance Raman and ^{31}P NMR Spectroscopy. Correlation between the Conformational Changes of the Protein and the Lipid Bilayer

Thomas Heimburg, Peter Hildebrandt,*,‡ and Derek Marsh*

Max-Planck-Institut für biophysikalische Chemie, Abteilung Spektroskopie, D-3400 Göttingen, Federal Republic of Germany

Received March 27, 1991; Revised Manuscript Received June 19, 1991

ABSTRACT: The interaction of cytochrome *c* with negatively charged lipids has been studied by resonance Raman spectroscopy of the protein heme group and ^{31}P NMR of the phospholipid headgroups. The gel-to-fluid-phase transition of dimyristoylphosphatidylglycerol induces shifts in the conformational and coordination equilibria of the bound cytochrome *c*, as recorded by the resonance Raman spectra in the fingerprint and marker band regions. Conformational and coordination shifts of the bound cytochrome are also induced on admixture of dioleoylglycerol or dioleoylphosphatidylcholine with dioleoylphosphatidylglycerol. In the case of dioleoylglycerol, significant changes take place even at levels as low as 5 mol %. Binding of cytochrome *c* induces or increases the content of near isotropically diffusing lipid registered by the ^{31}P NMR spectra of the different lipids studied. Admixture of dioleoylglycerol also increases the bilayer curvature of dioleoylphosphatidylglycerol, inducing an inverted hexagonal phase at 50 mol % concentration; the tendency to spontaneous curvature in the lipid appears to relax the conformational change detected in the protein.

Extrinsic proteins bind electrostatically at membrane surfaces, and these associations may have both a structural and a functional role. The peripheral interactions with negatively charged lipids, for instance, can affect both the conformation of the protein and the configuration of the membrane surface. One likely structural change for the lipid is an increase in local surface curvature, which in turn could favour the conformational change in the protein. In such a case, it is to be expected that the conformational effects may be enhanced by the presence of lipids, such as diacylglycerols (Das & Rand, 1986) or free fatty acids (Marsh & Seddon, 1982; Heimburg et al., 1990), which tend to increase the bilayer curvature.

It has been shown previously that two different conformational states, I and II, are induced on binding cytochrome *c* to negatively charged surfaces (Hildebrandt & Stockburger, 1989a,b), including anionic lipid dispersions (Hildebrandt et al., 1990). While the conformation of state I (cyt c_I^{3+})[1] is very similar to that in solution and the native six-coordinated low-spin configuration (6cLS) of the heme is preserved, in state II (cyt c_{II}^{3+}) the heme crevice opens and the iron exists in a thermal equilibrium between a five-coordinated high-spin (5cHS) and a new six-coordinated low-spin (6cLS) configuration. Since these latter structural changes are accompanied by a large negative shift of the redox potential, compared to state I, it is likely that they will be of direct relevance to the electron-transport function. On the other hand, it has also been shown that cytochrome *c* is capable of inducing inverted hexagonal phases in the inner mitochondrial membrane lipid cardiolipin (De Kruijff & Cullis, 1980).

In the present work, we have investigated the interaction of cytochrome *c* with negatively charged lipids alone, and with mixtures containing electroneutral and non-bilayer-forming lipids. Resonance Raman spectroscopy has been used as a probe of the protein conformation in the vicinity of the heme [for reviews, see Carey (1982); Kitagawa and Ozaki (1987); and Spiro (1988)] and broad-line ^{31}P NMR as a probe of the surface curvature of the phospholipid dispersions [see, e.g., Cullis and De Kruijff (1979)]. It is found both that cytochrome *c* increases the surface curvature of the lipid structures and that the conformational changes in the protein depend sensitively on the lipid composition and its phase state. In particular, low concentrations of diacylglycerol are found to be effective in modulating the conformational changes in the protein. The results of these model experiments indicate possible mechanisms for the surface activation of peripheral proteins, such as that of protein kinase C by diacylglycerols (Nishizuka, 1984, 1986) or of phospholipase A_2 by free fatty acids (Jain & Berg, 1989; Bell & Biltonen, 1989).

Materials and Methods

Materials. Cytochrome *c* (horse heart, type VI; Sigma, St. Louis, MO) was fractionated to remove deamidated forms according to Brautigan et al. (1978), converted completely to the ferric species with $K_3Fe(CN)_6$, and then dialyzed extensively against buffer solution (1 mM Hepes/1 mM EDTA, pH 7.5). Dimyristoylphosphatidylglycerol (DMPG) and dioleoylphosphatidylglycerol (DOPG) were obtained from Avanti Polar Lipids, Inc. (Pelham, AL). Oleic acid was obtained from Fluka (Buchs, Switzerland), and dioleoylphosphatidylcholine (DOPC) was from Sigma. Dioleoylglycerol (DOG) was prepared from DOPC by the action of phospholipase C (Boehringer-Mannheim, Mannheim, FRG). Lipid purity was checked by thin-layer chromatography.

Sample Preparation. Lipids were codissolved in CH_2Cl_2, the solvent was removed by a stream of nitrogen, and the lipid

‡Present address: Max-Planck-Institut für Strahlenchemie, Stiftstrasse 34-36, D-4330 Mülheim, FRG.

[1] Abbreviations: RR, resonance Raman; NMR, nuclear magnetic resonance; DMPG, 1,2-dimyristoyl-*sn*-glycero-3-phosphoglycerol; DOPG, 1,2-dioleoyl-*sn*-glycero-3-phosphoglycerol; DOPC, 1,2-dioleoyl-*sn*-glycero-3-phosphocholine; DOG, 1,2-dioleoyl-*sn*-glycerol; cyt c_I^{3+}, oxidized cytochrome *c* in conformational state I; cyt c_{II}^{3+}, oxidized cytochrome *c* in conformational state II; 6cLS, six-coordinated low spin; 5cHS, five-coordinated high spin; EDTA, ethylenediaminetetraacetic acid; Hepes, *N*-(2-hydroxyethyl)piperazine-*N'*-2-ethanesulfonic acid.

0006-2960/91/0430-9084$02.50/0

Table I: Concentration Ratios[a] at 22.5 °C for the Various Species of Cytochrome c Bound to Different Phospholipids and the Parameters of Protein Binding

lipid (mol/mol)	cyt c_{II}^{3+}/ cyt c_I^{3+}	ln (cyt c_{II}^{3+}5cHS/ cyt c_{II}^{3+}6cLS)	ΔG_b (kJ/mol)	N_m[b] (mol/mol)
DMPG	4.23 (4.4)	−2.83 (1.5)		8.4
DOPG	2.68 (9.1)	−2.75 (2.5)	−39	9.6
DOPG–DOG (70:30)	1.16 (16.1)	−2.25 (3.8)	−39	15.5
DOPG–DOPC (70:30)	0.69 (10.2)	−1.76 (4.4)	−37	25.8
OA–DOPC (30:70)	1.44 (3.6)	−2.29 (1.1)	−32	15.5

[a] The data are obtained from the band-fitting analysis described in the text. Standard deviations (in percent) are given in parentheses. [b] Molar ratio of charged lipids to cytochrome c at saturation protein binding.

mixture was then dried under vacuum for >3 h. For resonance Raman experiments, the dry lipids were dispersed in aqueous buffer (1 mM Hepes–1 mM EDTA, pH 7.5, or 1 mM sodium borate–1mM EDTA, pH 8.6, for the oleic acid containing samples). Complexes with cytochrome c were formed by adding the protein to the lipid suspension. Where necessary, the lipid dispersions were sonicated briefly in a bath sonicator. The final concentration of cytochrome c was 20 μM, and that of the lipid was 300 μM. Samples for NMR were prepared by gently hydrating 20 mg of negatively charged phospholipid in 0.2–0.5 mL of buffer (1 mM Hepes–1 mM EDTA, pH 7.5, or 1 mM sodium borate–1 mM EDTA, pH 8.6, for the oleic acid containing samples). When required, cytochrome c was then added to the lipid suspension. Samples containing unsaturated lipids were kept under nitrogen or argon during preparation and measurement.

Binding Studies. Samples were prepared with a constant lipid concentration (0.1 mM) and composition, but varying concentrations of cytochrome c. The lipid–protein complex was resolved by centrifugation (Ti-40 rotor, 45000 rpm), and the free cytochrome c concentration in the supernatant was determined spectrophotometrically.

Resonance Raman Experiments. RR spectra were excited at 407 nm by using the experimental arrangement described previously (Hildebrandt & Stockburger, 1989a,b). The laser power was 30 mW at the sample which was contained in a rotating cuvette to minimize photochemical degradation. The spectra were measured with a spectral slit width of 2.7 cm^{-1} and a step width of 0.2 cm^{-1}. They were accumulated by repetitive scanning (≈15 s per step) to a signal-to-noise ratio which was sufficient for band-fitting analysis. Further details of the experimental procedures can be found in Hildebrandt et al. (1990).

^{31}P NMR Spectroscopy. Proton dipolar decoupled ^{31}P NMR spectra were recorded at 6.3 T on a Bruker WH-270 spectrometer operating in the Fourier transform mode. Single 45° pulses of 6 μs were used with a recycle time of 4 s, together with 20-W broad-band gated proton decoupling. Chemical shifts were referred to external 85% phosphoric acid.

Results

Cytochrome c Binding. The binding curves of cytochrome c to dispersions of the different lipids were determined at a constant lipid concentration of 0.1 mM. The binding curves were typical of a single type of binding site. The curves were analyzed by a simple mass action model (effectively a Langmuir isotherm) to yield the molar free energy of binding per protein and the effective number of lipids per binding site. The values obtained by fitting are given in Table I. The free energy of binding does not differ greatly between the different lipid systems, but the binding stoichiometry changes steeply on going from the pure negatively charged lipid systems to the mixtures with neutral or zwitterionic lipids. In each case, the binding is strong, ensuring that all the protein is bound to the lipid under the conditions used for the RR experiments. The one exception is with the mixture 70% DOPG + 30% DOPC in which the RR spectra had to be corrected for the unbound protein.

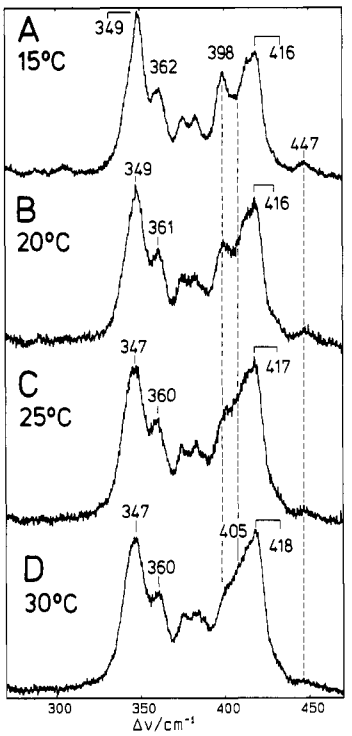

FIGURE 1: Resonance Raman spectra of cytochrome c^{3+}–DMPG in the low-frequency region, recorded at different temperatures: (A) 15 °C; (B) 20 °C; (C) 25 °C; (D) 30 °C. The excitation line was at 407 nm.

Resonance Raman Measurements. The RR spectra were recorded in the marker band (1325–1525 cm^{-1}) and fingerprint (270–470 cm^{-1}) regions and were analyzed by an iterative band-fitting routine. For these spectral regions, the RR bands of the three cytochrome states, cyt c_I^{3+}6cLS, cyt c_{II}^{3+}6cLS, and cyt c_{II}^{3+}5cHS, have been identified and the frequencies, ν_{ij}, half-widths, $\Delta\nu_{ij}$, and intensity ratios, R_{ij}, determined (Hildebrandt et al., 1990). The intensity ratios (R_{ij}) of a component j relate the different RR bands, i, to a given reference band. Thus, in a first approximation, the measured RR spectra were fitted by a superposition of the whole spectra of the individual species, rather than by independent single Lorentzian profiles. A subsequent refinement of the fits was then performed by progressively releasing the restraints on the spectral parameters ν_{ij}, $\Delta\nu_{ij}$, and R_{ij}, which were varied over a limited range in order to optimize these parameters for each spectrum.

Figure 1 shows the temperature dependence of the RR spectra of cytochrome c^{3+}–DMPG in the low-frequency (fingerprint) region. Changes are seen in the spectra with increasing temperature, particularly between 20 and 25 °C in the region of the lipid-phase transition. The most pronounced effects are on the bands between 398 and 418 cm^{-1}. While at 15 and 20 °C the band at 398 cm^{-1} which originates from cyt c_I^{3+}6cLS is clearly observable, its intensity decreases at 25 and 30 °C. This is paralleled by an increase in intensity

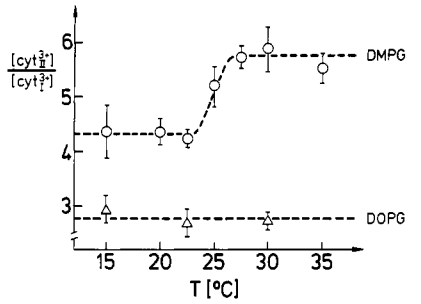

FIGURE 2: Temperature dependence of the conformational equilibrium constant for cyt c_{II}^{3+} and cyt c_I^{3+} bound to DMPG (O) and to DOPG (Δ).

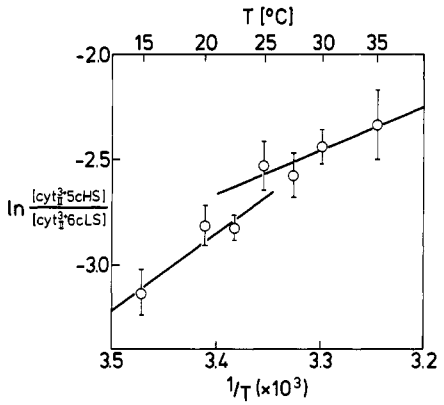

FIGURE 3: van't Hoff plot for the temperature dependence of the coordination equilibrium (5cHS/6cLS) in cytochrome c^{3+} bound to DMPG.

Table II: Thermodynamic Parameters for the Coordination Equilibrium cyt c_{II}^{3+}6cLS ⇌ cyt c_{II}^{3+}5cHS of Cytochrome *c* in State II Bound to Phospholipid Dispersions

lipid, phase	ΔH (kJ/mol)	ΔS (J mol^{-1} K^{-1})
DMPG, gel	−31.0	−126
DMPG, fluid	−17.0	−66
DOPG, fluid	−20.5	−92

in the region around 405 cm^{-1}, which is due to the bands of cyt c_{II}^{3+}6cLS and cyt c_{II}^{3+}5cHS (Hildebrandt et al., 1990). The temperature-dependent changes were quantitated by band-fitting analysis of the spectra in both the fingerprint (270–470 cm^{-1}) and marker band (1325–1525 cm^{-1}) regions of the spectrum. The relative intensities of the 8–12 diagnostic bands were then converted into relative concentrations of the 3 different cytochrome *c* species, as described previously (Hildebrandt et al., 1990).

The temperature dependence of the cyt c_{II}^{3+}:cyt c_I^{3+} ratio (here cyt c_{II}^{3+} includes both spin configurations) is given in Figure 2. This ratio remains essentially constant at a value of 4.3 below the lipid gel–fluid-phase transition, and increases at 25 °C to a value of approximately 5.8 above the phase transition. A small decrease in ratio at higher temperature (35 °C) cannot be excluded, within the experimental accuracy of the data. These results indicate that the conformational state II is preferentially stabilized by the fluid phase of DMPG. The data for the temperature dependence of the coordination equilibrium are given in a van't Hoff plot of the cyt c_{II}^{3+}-5cHS:cyt c_{II}^{3+}6cLS ratio in Figure 3. The values of the enthalpy and entropy for the coordination change cyt c_{II}^{3+}6cLS ⇌ cyt c_{II}^{3+}5cHS, both above and below the gel-to-fluid-phase transition of DMPG, are given in Table II.

Sections of the RR spectra of the marker band and fingerprint regions of cytochrome c^{3+}–DOPG are given together with the band-fitting analysis in Figure 4A,B. Here the bands

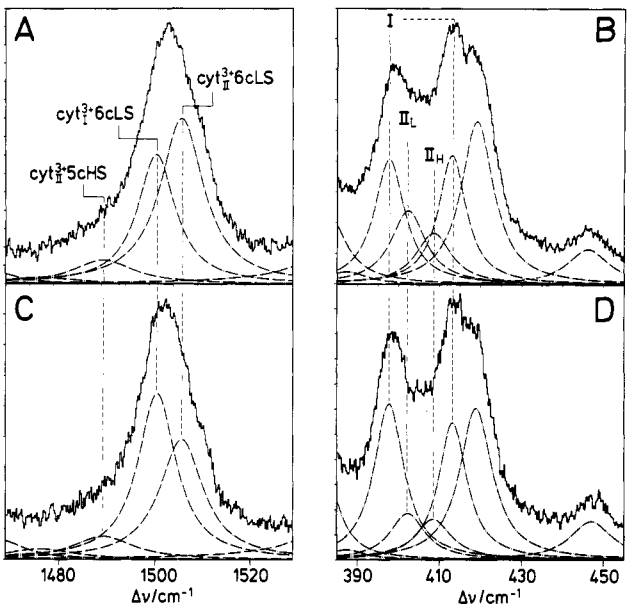

FIGURE 4: Resonance Raman spectra of (A, B) cytochrome c^{3+}–DOPG and (C, D) cytochrome c^{3+}/DOPG–DOG (9:1 mol/mol) excited at 407 nm (T = 22.5 °C). The dotted lines are the fitted Lorentzian profiles.

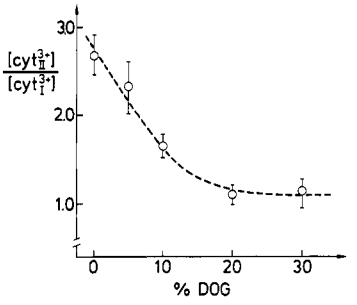

FIGURE 5: Concentration ratio of cyt c_{II}^{3+} and cyt c_I^{3+} in cytochrome c^{3+}/DOPG–DOG, as a function of DOG content. T = 22.5 °C.

attributable to cyt c_I^{3+}6cLS are considerably stronger, relative to those from cyt c_{II}^{3+}6cLS and cyt c_{II}^{3+}5cHS, than was found for cytochrome c^{3+}–DMPG (cf. Table I). Furthermore, the cyt c_{II}^{3+}:cyt c_I^{3+} ratio remains essentially constant between 15 and 30 °c, corresponding to the lack of a phase transition in this temperature range for DOPG (see Figure 2). However, we note a slight increase in intensity of the marker bands of cyt c_{II}^{3+}5cHS, at the expense of the 6cLS configuration. The results of a van't Hoff analysis of the temperature dependence for the coordination equilibrium in cytochrome c^{3+}–DOPG are given in Table II.

In a similar manner, the effect on the conformation of bound cytochrome *c* of mixing different electroneutral lipids with the negatively charged lipids (DOPG or OA) was investigated. The RR spectra of the marker band and fingerprint regions of cytochrome c^{3+}/DOPG–DOG (9:1 mol/mol) are given in Figure 4C,D. Compared with DOPG alone, the spectra are dominated by the bands arising from cyt c_I^{3+}. The results of the band-fitting analysis for the spectra of cytochrome c^{3+} bound to different DOPG–DOG mixtures are shown for the conformational equilibrium in Figure 5. Progressive admixture of the neutral lipid DOG in DOPG bilayers leads to a reduction in the cyt c_{II}^{3+} content to a limiting value at 30 mol % DOG, corresponding to a conformational ratio cyt c_{II}^{3+}/cyt c_I^{3+} ≈ 1.

Admixture of the zwitterionic lipid DOPC has an even greater effect on the conformational equilibrium of the bound

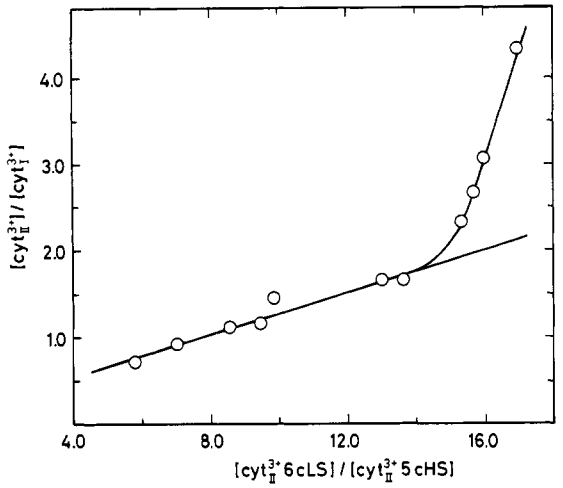

FIGURE 6: Correlation of the equilibrium constants for the coordination transition in state II ([cyt c_{II}^{3+}6cLS]/[cyt c_{II}^{3+}5cHS]) and the conformational transition ([cyt c_{II}^{3+}]/[cyt c_{I}^{3+}]). Data from all the different lipid systems are at T = 22.5 °C. The linear region in the first part of the plot has an intercept at −1 on the abscissa.

cytochrome c^{3+} than that caused by DOG. The fractional population of cyt c_{II}^{3+} is reduced from 75% to approximately 40% with 30 mol % DOPC, compared to 55% with the same percentage of DOG (Table I). On the other hand, in a mixture containing only 30 mol % negatively charged OA with 70 mol % DOPC, the content of state II is reduced only to 60% (Table I).

A correlation diagram of the conformational and coordination equilibria at constant temperature (22.5 °C) is given for cytochrome c^{3+} bound to each of the different lipid systems in Figure 6.

^{31}P NMR Spectroscopy. The broad-line ^{31}P NMR spectra of coarse dispersions of DOPG–DOG mixtures, in the presence and the absence of saturating quantities of cytochrome c^{3+}, are given in the upper part of Figure 7. In the absence of protein, the spectra consist of axial powder patterns, characteristic of a lamellar lipid arrangement, for DOG contents up to 20 mol %. At 30 mol % DOG (not shown), the spectrum is dominated by an isotropic peak, with possible underlying lamellar and nonlamellar powder patterns. At 50 mol % DOG, the spectrum is dominated by an axial powder pattern of smaller anisotropy with reversed sign, characteristic of a cylindrical structure, such as the inverted hexagonal phase. In the presence of excess cytochrome c^{3+}, a strong isotropic peak appears in all the spectra, with underlying axial powder patterns similar to those obtained in the absence of protein.

Corresponding ^{31}P NMR spectra for other mixtures of negatively charged and neutral lipids are given in the lower part of Figure 7. For both DOPG–DOPC (70:30 mol/mol) and OA–DOPC (30:70 mol/mol), spectra characteristic of extended lamellae are obtained in the absence of protein. In the presence of an excess of cytochrome c^{3+}, an isotropic peak is superimposed on the lamellar powder pattern, but to a lesser extent than in the presence of diacylglycerol.

Discussion

The results presented here show that binding to negatively charged lipid surfaces shifts the conformational and coordination equilibria of cytochrome c^{3+}. The extent of displacement in the protein equilibrium is strongly dependent on the conformational state of the lipid and on its composition. At the same time, perturbations of the lipid surfaces are caused by binding of the protein, resulting in an increased local surface curvature. These aspects are discussed separately below.

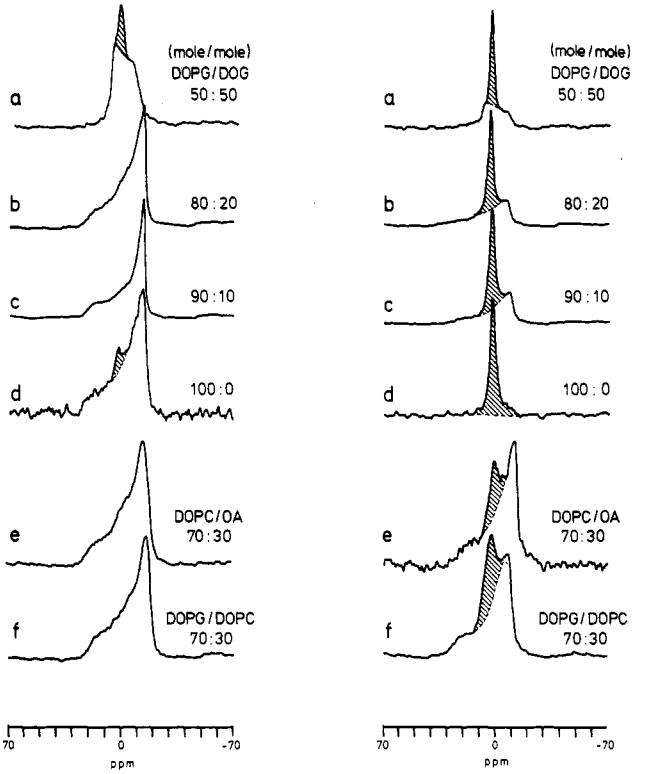

FIGURE 7: 109-MHz proton dipolar decoupled ^{31}P NMR spectra of lipid mixtures in the presence (right-hand side) and in the absence (left-hand side) of (excess) cytochrome c^{3+}. (a) DOPG/DOG 50:50 mol/mol; (b) DOPG/DOG 80:20 mol/mol; (c) DOPG/DOG 90:10 mol/mol; (d) DOPG; (e) DOPC/OA 70:30 mol/mol; (f) DOPG/DOPC 70:30 mol/mol mixtures. T = 22 °C. The isotropic spectral component is indicated by hatching.

Structural Changes in Cytochrome c. The conformational states I and II, characterized previously for cytochrome c^{3+} bound to negatively charged surfaces (Hildebrandt & Stockburger, 1989a,b), are also stabilized in anionic lipid vesicle systems. In state I, the native structure is very similar to that of cytochrome c^{3+} in aqueous solution, whereas in state II the heme crevice opens, reducing the steric constraints of the protein matrix on the heme and reducing the hydrophobicity of its environment. The electrostatic interaction between the positively charged lysine residues surrounding the heme crevice and the negatively charged lipid headgroups controls the conformational equilibrium between states I and II, as well as the coordination equilibrium in state II, in a manner similar to that at other negatively charged surfaces [cf. Hildebrandt and Stockburger (1989a,b)]. The lipid system is different from those of the previous studies in that it has the freedom to adjust its surface curvature [see, e.g., Seddon (1990)] to match the charge distribution on the protein. This gives rise to a strong dependence of the protein conformational equilibria on lipid composition, especially for those lipids such as diacylglycerol which tend to give rise to spontaneous curvature [cf. Tate et al. (1991)]. The results of Figure 5 clearly indicate that the conformational population of state II is strongly reduced by rather low concentrations of dioleoylglycerol.

The physical state of the lipid may also have a considerable influence on the conformational equilibrium, as seen in Figure 2. The proportion of conformational state II increases on going from the gel to the fluid phase for DMPG, and in both phases is greater than in the fluid phase of DOPG. Since, in the absence of specific ion binding effects, the lipid surface charge density is expected to be greater in the gel phase than in the fluid phase of DMPG and yet smaller in the fluid phase of

DOPG, it seems that there is some other effect contributing to the electrostatic control of the conformational equilibrium. It is most likely that this is the distribution of charges, i.e., that the charge separation should match that of the positively charged residues on the cytochrome *c* molecule. The results with the DOPG–DOG system discussed above suggest that this can be most readily achieved by a redistribution of the different components in lipid mixtures.

Thermodynamically, the two conformations are expected to have different binding energies. The composite association constant for both conformations, K_{tot}, that is measured experimentally in the binding determinations is related to the association constants for the individual conformations by the identities:

$$K_{tot} = K_I(1 + K_{II/I}) \quad (1)$$

$$K_{tot} = K_{II}(1 + 1/K_{II/I}) \quad (2)$$

where K_I and K_{II} are the association constants for conformations I and II, respectively, and $K_{II/I}$ is the equilibrium constant for the conformational change cyt c_{II}^{3+}/cyt c_I^{3+}. The difference in binding free energy between conformation I and conformation II is therefore given by

$$\Delta G_I - \Delta G_{II} = -RT \ln [(1 + 1/K_{II/I})/(1 + K_{II/I})] \quad (3)$$

where R is the ideal gas constant and T the absolute temperature. At 22.5 °C, this difference in binding free energy ranges from approximately 3.5 kJ/mol (4.5 kJ/mol in the fluid phase) for DMPG to −0.9 kJ/mol for the DOPG–DOPC 70:30 mol/mol mixture (cf. Table I). For the DOPG–DOG 70:30 mol/mol mixture, the binding free energies of the two conformations differ by less than 0.5 kJ/mol. For the OA–DOPC 30:70 mol/mol mixture, the difference in binding free energy between the two conformations is only 0.9 kJ/mol. Therefore, the somewhat weaker total binding for this latter mixture (see Table I) does not correspond to a preferential binding for one of the two conformations.

The lipid-induced changes in conformational equilibria might be expected to be expressed also in corresponding changes in the coordination equilibria. In Figure 6, this is found to be the case, where data from all the different lipid systems, at 22.5 °C, are collected together. The content of the 6cLS state is found to increase strongly as the fraction of the conformational state II increases in response to the changes in the lipid composition. Interestingly, the initial part of the dependence in Figure 6 is found to be approximately linear, with an intercept at −1 on the *x* axis. Due to their cyclical nature, the conformational and coordination equilibria are related by the identity:

$$K_{II/I} = K_{HS/I}(1 + K_{LS/HS}) \quad (4)$$

where $K_{LS/HS}$ (=$1/K_{HS/LS}$) and $K_{HS/I}$ are the equilibrium constants referring to the cyt c_{II}^{3+}6cLS/cyt c_{II}^{3+}5cHS and cyt c_{II}^{3+}5cHS/cyt c_I^{3+} equilibria, respectively. Hence, it would appear that the cyt c_{II}^{3+}5cHS/cyt c_I^{3+} equilibrium constant remains approximately constant at a value of $K_{HS/I} = 0.12$ in the first phase of the plot. In the second part of the plot [corresponding to lipid systems with a considerably smaller tendency to spontaneous curvature (Cevc & Marsh, 1987)], $K_{HS/I}$ clearly no longer remains constant but increases considerably for these lipid systems. The conjugate equilibrium constant (cyt c_{II}^{3+}6cLS/cyt c_I^{3+}) does not display a constant region and changes continuously between the different lipid systems.

The temperature dependence of the coordination equilibria also gives evidence for the sensitivity to the state of the lipid. The ratio cyt c_{II}^{3+}5cHS/cyt c_{II}^{3+}6cLS increases in the interval from 15 to 30 °C, with an enthalpy and entropy for the change in coordination state that are given in Table II. The values are in the same range as those for the 6cLS/5cHS equilibrium in microsomal cytochrome P-450 (Cinti et al., 1979). The van't Hoff plots for DMPG reveal thermodynamically distinct behavior above and below the gel-to-fluid-phase transition at 23 °C (Figure 3). The entropy and enthalpy above the transition are reasonably close to those of DOPG in the fluid phase, suggesting that lipids in the gel and fluid phases induce a qualitatively different temperature dependence of the coordination equilibrium.

Comparison of Figures 2 and 5 reveals different effects of the increase in chain flexibility on chain melting of DMPG from those of the addition of DOG to DOPG on the cyt c_{II}^{3+}/cyt c_I^{3+} equilibria. The ^{31}P NMR spectra (Figure 7 and see below) demonstrate that increasing content of DOG has the tendency to induce spontaneous curvature [cf. Gruner (1985)] in the lipid bilayer in the absence of cytochrome *c*, resulting ultimately in the formation of an inverted hexagonal phase at 50 mol % DOG. Therefore, whereas in the absence of DOG the protein has to adapt to the lipid surface structure and the cyt c_{II}^{3+} conformation is favored, in the presence of DOG the fluctuations in surface curvature allow the protein to relax more to the cyt c_I^{3+} conformation which is close to its native structure in solution. This control by the membrane curvature represents a fundamental difference from the situation with cytochrome *c* bound to totally stiff electrodes [cf. Hildebrandt and Stockburger (1989a)]. The transition of DMPG from the gel to fluid phase is also expected to increase the surface flexibility of the bilayer, but it is seen nevertheless to give rise to an increase in conformational state II rather than state I of the bound cytochrome (Figure 2). Whereas we have no final explanation for this observation, it seems plausible that the conformational state of the bound protein is dominated by the spatial distribution of the headgroup charges in the DMPG bilayers, for which the molecular packing is tighter than in the case of DOPG. In both the gel and fluid states of DMPG, the majority of the cytochrome c^{3+} is in state II (80% and 85%, respectively), indicating a strong control of the conformational state by interaction with the headgroup charge distribution in the saturated lipid bilayers.

Structural Changes in the Lipid. The ^{31}P NMR spectra are sensitive to the surface curvature of the different lipid aggregate structures. Isotropic curvature gives rise to a complete averaging of the spectral anisotropy, if the translational diffusion of the phospholipid molecules around the curved surfaces is sufficiently rapid (Cullis & De Kruijff, 1979; Knowles & Marsh, 1991). Either cubic lipid phases, small spherical vesicles, or extended bilayers with high local surface curvature can give rise to isotropic spectra. Lipid phases with cylindrical symmetry, on the other hand, give rise to spectra with a very characteristic degree of anisotropy. In the present work, it is found that whereas the effect of adding increasing amounts of DOG is to induce an inverted hexagonal lipid phase [cf. Das and Rand (1986)], the binding of cytochrome *c* has the general effect of producing isotropic lipid components (Figure 7). This can be interpreted as an increase in surface curvature of the lipid aggregates, induced in the region of the protein binding.

It is interesting to correlate this change in the surface curvature with the stoichiometries of the lipid association obtained from the binding assays (see Table I). The introduction of uncharged or zwitterionic lipids is seen to decrease the maximum extent of protein binding, even when this is referred to the amount of charged lipid. The binding energy

only changes appreciably, however, in the case of the OA–DOPC (30:70 mol/mol) system. This suggests that an inhomogeneous distribution of the different lipids is induced on binding the protein. Asymmetry of the lipid distribution across the two halves of the bilayer is one possible form of inhomogeneity that would favor the increase in curvature of the lipid surface, which is evidenced by the NMR results.

Implications for Other Systems. There are at least two well-documented cases for which the activity of peripheral membrane-associated enzymes is modulated by lipid composition. Protein kinase C binds to negatively charged lipids (e.g., phosphatidylserine), and its activity is controlled by diacylglycerols (Nishizuka, 1984, 1986). The diacylglycerol concentration in natural membranes is very low, but is increased for a finite period during phosphatidylinositol turnover (Berridge, 1984). The data presented here demonstrate that even small admixtures of diacylglycerol can give rise to significant conformational changes in one particular peripheral membrane protein, viz., cytochrome *c*. On the other hand, Epand et al. (1988) have also shown that lipids other than diacylglycerol which potentiate inverted hexagonal lipid-phase formation can also promote activation of protein kinase C.

Different species of the lipolytic enzyme phospholipase A_2 bind either to charged or to uncharged lipid surfaces. The presence of the hydrolytic lipid products (fatty acids and lysolipids) is required for full activation of the enzyme (Bell & Biltonen, 1989; Jain & Berg, 1989). Calculations based on a hydrolysis product dependent change in equilibrium between an active and inactive form of the enzyme are consistent with the observed activation pattern (Biltonen et al., 1990). In the present work, we have demonstrated directly that admixture of fatty acids can also result in conformational changes of membrane-bound cytochrome *c*.

It is probable that the above results may be of considerably greater generality. Peripheral proteins may often be poised in a conformational equilibrium susceptible to switching between states of different activity or function. The membrane lipids are heterogeneous in composition, comprising species with greater or lesser tendency toward spontaneous membrane curvature [cf. Hui and Sen (1989)]. A reciprocal thermodynamic relation between the states of both lipid and protein is therefore to be expected, leading to a general mechanism of membrane activation by lipid–protein interaction.

Registry No. Cyt *c*, 9007-43-6; DOPG, 62700-69-0; DOPC, 4235-95-4; DOG, 24529-88-2; DMPG, 18194-24-6; Fe, 7439-89-6; oleic acid, 112-80-1.

References

Bell, J., & Biltonen, R. L. (1989) *J. Biol. Chem. 264*, 12194–12200.

Berridge, M. J. (1984) *Biochem. J. 220*, 345–360.

Biltonen, R. L., Heimburg, T. R., Lathrop, B. K., & Bell, J. D. (1990) in *Biochemistry, Molecular Biology and Physiology of Phospholipase A_2 and its Regulatory Factors* (Mukherjee, A. B., Ed.) pp 85–104, Plenum Press, New York.

Brautigan, D. L., Ferguson-Miller, S., & Margoliash, E. (1978) *Methods Enzymol. 53D*, 128–164.

Carey, P. R. (1982) *Biochemical Applications of Raman and Resonance Raman Spectroscopy*, Academic Press, New York.

Cevc, G., & Marsh, D. (1987) *Phospholipid Bilayers. Physical Principles and Models*, 443 pp, Wiley-Interscience, New York.

Cinti, D. L., Sligar, S. G., Gibson, G. G., & Schenkman, J. B. (1979) *Biochemistry 18*, 36–42.

Cullis, P. R., & De Kruijff, B. (1979) *Biochim. Biophys. Acta 559*, 399–420.

Das, S., & Rand, R. P. (1986) *Biochemistry 25*, 2882–2889.

De Kruijff, B., & Cullis, P. R. (1980) *Biochim. Biophys. Acta 601*, 235–240.

Epand, R. M., Stafford, A. R., Cheetham, J. J., Bottega, R., & Ball, E. H. (1988) *Biosci. Rep. 8*, 49–54.

Gruner, S. M. (1985) *Proc. Natl. Acad. Sci. U.S.A. 82*, 3665–3669.

Heimburg, T., Ryba, N. J. P., Würz, U., & Marsh, D. (1990) *Biochim. Biophys. Acta 1025*, 77–81.

Hildebrandt, P., & Stockburger, M. (1989a) *Biochemistry 28*, 6710–6721.

Hildebrandt, P., & Stockburger, M. (1989b) *Biochemistry 28*, 6722–6728.

Hildebrandt, P., Heimburg, T., & Marsh, D. (1990) *Eur. Biophys. J. 18*, 193–201.

Hui, S.-W., & Sen, A. (1989) *Proc. Natl. Acad. Sci. U.S.A. 86*, 5825–5829.

Jain, M. K., & Berg, O. G. (1989) *Biochim. Biophys. Acta 1002*, 127–156.

Kitagawa, T., & Ozaki, Y. (1987) *Struct. Bonding 64*, 71–114.

Knowles, P. F., & Marsh, D. (1991) *Biochem. J. 274*, 625–641.

Marsh, D., & Seddon, J. M. (1982) *Biochim. Biophys. Acta 690*, 117–123.

Nishizuka, Y. (1984) *Nature (London) 308*, 693–698.

Nishizuka, Y. (1986) *Science 233*, 305–311.

Seddon, J. M. (1990) *Biochim. Biophys. Acta 1031*, 1–69.

Spiro, T. G., Ed. (1988) *Biological Applications of Raman Spectroscopy*, Vol. III, Wiley, New York.

Tate, M. W., Eikenberry, E. F., Turner, D. C., Shyamsunder, E., & Gruner, S. M. (1991) *Chem. Phys. Lipids 57*, 147–164.